Journal of Hydroscience and Hydraulic Engineering
Vol. 29, No.1 May, 2011, 57-68

COUPLING A HYDRAULIC MODEL INCORPORATING RIVER CROSS-SECTIONAL GEOMETRY DERIVED FROM HIGH RESOLUTION DSM WITH A HYDROLOGICAL MODEL FOR RIVER DISCHARGE ESTIMATION

By

Wenchao Sun

Interdisciplinary Graduate School of Medicine and Engineering, University of Yamanashi, Japan

Hiroshi Ishidaira

Interdisciplinary Graduate School of Medicine and Engineering, University of Yamanashi, Japan

and

Satish Bastola

National University of Ireland, Maynooth, Co. Kildare, Ireland

SYNOPSIS

A variety of hydraulic information can be obtained from space nowadays, which are potentially useful for river discharge estimation. In this study, river cross-sectional geometry was extracted from high resolution Digital Surface Model (DSM) which is produced from ALOS PRISM images. Then the derived information was integrated with Manning Equation to describe the relation between discharge and cross-sectional water surface width. By integrating a rainfall-runoff model with this relation which is used to describe hydraulic relation at basin outlet, it is possible to calibrate the rainfall-runoff model using satellite observations of river width. Such methodology is demonstrated by means of a case study in the Mekong River at Pakse. The results show that discharge is estimated with acceptable accuracy and values of the hydraulic relation parameters obtained from calibration properly reflect hydraulic condition at Pakse region. The method proposed in this study could be an effective approach for estimating discharge in large ungauged basins.

INTRODUCTION

As a major link between the continents and the oceans, river discharge is an important component in the global hydrologic and biochemical cycles. River discharge deposits huge amounts of particulates and dissolved material into the oceans, which have important impact on ocean chemistry. From the terrestrial aspect, it is a major source of the natural water available for humans and also regulates ecological cycles. There is a general consensus that the reliable prediction of freshwater resources availability should be based on the comprehensive measurements of surface water (1). River discharge data provides important information which is of great benefit to both society and science. However, gauging stations and access to river discharge information have decreased since 1980s (2).

Table 1 The empirical relations being used for discharge estimation from space in past studies*

	Equations
Single variable	$W_e=aQ^b$ (5)
	$Q=c(H_s-H_0)^d$ (6)
Multiple variables	$Q=k_1 \cdot W_e^e \cdot Y^f \cdot S^g$ (7)
	$Q=k_2 \cdot W_e^h \cdot V^i \cdot S^j$ (7)
	$Q=k_3 \cdot W_e^k \cdot V^l$ (7)
	$Q=k_4 \cdot W^{*m} \cdot Y^{*m} \cdot Y^o \cdot S^p$ (7)
	$Q=qW_e^r \xi^s$ (8)

*Q is discharge, W_e is water surface width, H_s is water surface elevation, H_0 is elevation of effective zero flow, Y is mean depth, S is slope, W^* is bankfull width, Y^* is bankfull mean depth, ξ is channel sinuosity, and a to s are empirical parameters

Hydrographic data obtained from satellites offer the possibility of broad and potentially frequent global coverage of river discharge estimates (3). Due to improvements in remote sensing, river cross-sectional water surface width, water level, water surface slope, river channel sinuosity can be observed from space. As flow width, depth and velocity can not be measured from satellite simultaneously, functions correlating discharge to one or more measurable variables are necessary for the purpose of river discharge estimation (4). Table 1 summarizes the relations adopted in researches estimating discharge from space. The parameters in these rating functions are empirical ones that reflect river cross-sectional geometry and balance between gravity and friction, for which calibration based on discharge data is necessary to identify these parameters. The reliance on observed discharge data limits applications of this approach to ungauged sites.

The Manning Equation describes a well known relation for water flow estimation in open channel condition. It is more physically based than the empirical relations in Table 1, for which river width or water surface elevation is indispensable for scaling cross-sectional area that water flow occupies. If information about river channel cross-sectional shapes and slope–resistance relations are available, based on the Manning Equation, river discharge can be computed from satellite observations of either of the two hydraulic variables. The advantage is that the need of discharge data for calibration is eliminated. Nowadays, the high resolution Digital Elevation Model (DEM) and the Digital Surface Model (DSM) can be produced from Light Detection and Ranging (LiDAR) data and stereo pairs of aerial photos and satellite images. The Panchromatic Remote-sensing Instrument for Stereo Mapping (PRISM), which is loaded on the Advanced Land Observing Satellite (ALOS) launched by Japan in 2006, was designed to generate worldwide topographic data with respect to its high resolution (9). The Digital Surface Model (DSM) provided by Remote Sensing Technology Center of Japan (RESTEC) has a spatial resolution of 2.5 meter. By means of this high solution DSM, the cross section geometry of large rivers could be obtained, which provides useful information for discharge estimation from remote sensing.

The purpose of this study is to propose a new approach for long time series of discharge estimation at daily scale in ungauged basins where in situ discharge gauging is unavailable. The cross-sectional geometry derived from ALOS PRISM DSM was combined with Manning Equation to describe relation between discharge and cross-sectional water surface width (Q-W_e relation). By integrating the Rainfall-Runoff model (RR model) with this Q-W_e relation which is adopted to describe hydraulic relation at basin outlet, instead of discharge data, the RR model is calibrated against satellite observations of river width by an automatic calibration algorithm. Compared with Sun *et al.* (10) using at-a-station hydraulic geometry to the describe Q-W_e relation, which was also adopted to calibrate RR model against river width, one advantage of this method is that the parameters of the Manning Equation based relation are

physically meaningful or can be set according to literature value, which facilitates setting robust ranges of parameters before automatic calibration. Furthermore, setting proper ranges is important to reduce the uncertainty in the calibration process, which could be further reduced, if the values of physically based parameters are determined by field surveys.

METHODOLOGY

Combining river cross-sectional geometry information derived from PRISM DSM data with Manning Equation

The Manning Equation is a widely used empirical formula for estimating river discharge in open channel flow conditions driven by gravity:

$$Q = \frac{1}{n} \times R^{2/3} \times S^{1/2} \times A \tag{1}$$

where n is the Manning roughness coefficient; S is the slope; R is the hydraulic radius; and A is the river cross-sectional area that flow occupied. River water surface width (W_e) can be observed with widely spatial and temporal coverage from remote sensing. If information about river cross-sectional shape is available, the values of R and A corresponding to specific value of W_e can be obtained. Thus if values of n and S are known, discharge can be calculated. The motivation for using cross-sectional shape derived from PRISM DSM is to make W_e as an index for scaling R and A.

PRISM DSM provides the Earth's surface elevation at a high spatial resolution of 2.5m. The value of elevation provided by the DSM data is in the form of integer. Water surface is treated as "dead area" and no elevation is provided. To the end of scaling R and A using W_e, several steps are necessary:

1. Building the relation between river cross-sectional width (W) and corresponding elevation (H) above water surface. As shown in Fig.1 (a), the elevations of the portion of cross section above water surface can be obtained in 2.5 meter horizontal interval. Based on this information, the horizontal distance between points with the same elevation is derived. From this distance for each elevation above water surface, the *W-H* relation is established.

2. Extending the *W-H* relation to the whole cross-section. As the shape below water surface can not be obtained from DSM, we assume the bottom of cross section is flat. By means of extrapolation from *W-H* relation derived in Step one and proper estimation about elevation of effective zero flow (H_0) which represents the elevation of the flat bottom, the *W-H* relation for the whole cross-section is built.

3. Building the relation between W_e and R, W_e and A. Based on the *W-H* relation, under assumption that shape between each two adjacent integer elevations is symmetrical trapezoid as shown in Fig.1 (b), quantitive relations between cross-sectional width and other factors describing cross section geometry, such as cross-sectional area, can be obtained. Then R and A corresponding to satellite observations of W_e can be calculated.

Combined with information about cross-sectional geometry derived from PRISM DSM, Eqs. 1 is converted into a new form:

$$Q = \frac{1}{n} \times \left[f_1(W_e|H_0) \right]^{2/3} \times S^{1/2} \times f_2(W_e|H_0) \tag{2}$$

where f_1 and f_2 is the W_e-R and W_e-A relation derived from PRISM DSM respectively; n, S and H_0 are three parameters that values need to be specified.

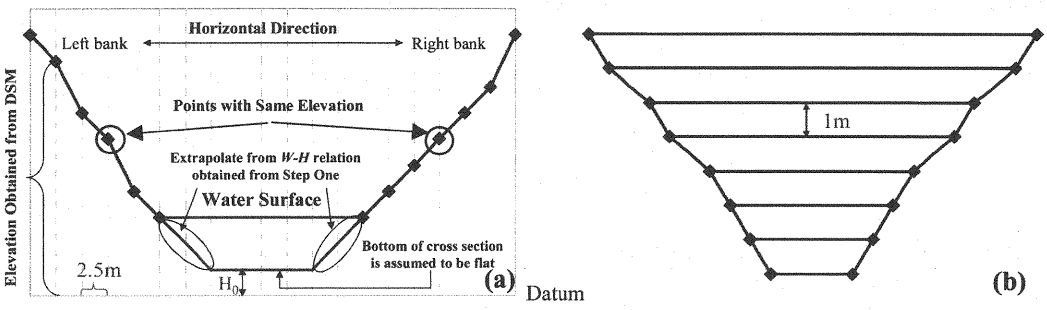

Fig. 1 (a) The schematic description of deriving the relation between the cross-sectional width and the corresponding elevation from DSM data. (b) The geometrical model describing the cross-section shape which consists of a series of symmetrical trapezoids

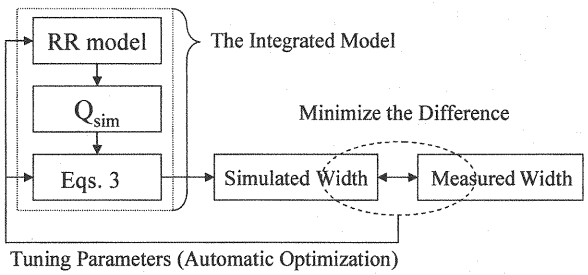

Fig. 2 The integrated model and calibration scheme

Integrating RR model with PRISM DSM data based Manning Equation

Obtaining reasonable values of the three parameters in Eqs. 2 is challenging. n is usually estimated by modeler subjectively, which is one major source of error for discharge estimation using the slope-area method (4). S and H_0 can be measured from field survey. However, as our target areas are ungauged basins, direct observations are relatively difficult. To reduce uncertainty associated with estimating values of the three parameters, in this study, we did not use Eqs. 2 in the straightforward manner as mentioned above.

The RR model is widely used for river discharge estimation. The reliance on discharge data for calibration limits direct applications in ungauged basins. For RR models, output is simulated discharge at the basin outlet. For inverse function of Eqs. 2, W_e is expressed as:

$$W_e = f(Q|H_0, n, S) \tag{3}$$

where Q is input of Eqs. 3; W_e is output, and n, S and H_0 are the three parameters. A physical explanation is that variation of discharge is accompanied by change of river width. By integrating the RR model with Eqs. 3, which is adopted to describe the Q-W_e relation at the basin outlet, water surface width corresponding to the simulated discharge by means of the RR model is computed by Eqs. 3. In the sense, river width becomes the output of the integrated model (i.e., the RR model combined with Eqs. 3). For basins discharge gauging is unavailable at the basin outlet, but in the cases of satellite observations of the river width, this integrated model can be calibrated directly. Also the

calibration objective is shifted to minimize the difference between satellite measurements and simulated values, which is achieved by tuning parameters of RR model and Q-W_e relation simultaneously. And no discharge data are needed under this calibration scheme which is shown in Fig. 2. After calibration, we consider the parameters for the RR model being properly identified. Finally, the calibrated RR model alone will be utilized for estimating discharge for the same period as calibration.

Under the proposed calibration scheme, the n, S and H_0 are considered to be time-invariants as RR model's parameters. And the cross-sectional geometry at the basin outlet derived from DSM is thought to be constant for the whole calibration period. Therefore, to reduce uncertainty associated with incorporating Eqs. 3, this method is only applicable to basins for which cross-sectional shape at the basin outlet does not change dramatically. For measuring river width from remote sensing, to reduce the error associated with spatial resolution of satellite images, large rivers are preferred.

APPLICATION EXAMPLE

Study area and calibration data

The study area is the Mekong River at Pakse which is located in the southwest part of Laos. The Pakse gauging station (15°07'N, 105°48'E) is at the confluence of the Xedone and Mekong Rivers. Minimum and maximum discharge for the period of 1923-2005 is 1,060m^3/s and 57,800m^3/s respectively. The whole upstream area of Pakse station (545,000 km^2) is selected as the target area for rainfall-runoff simulation. We obtained 16 scenes of Japanese Earth Resources Satellite-1(JERS-1) Synthetic Aperture Radar (SAR) images over the Pakse region, which cover the period of 1995-1998. On SAR images, the water surface area takes on low brightness, due to low backscattering. For each image, spatially averaged river width was estimated by dividing the water surface area in the Pakse region obtained through visual interpretation by the reach length (refer to Sun *et al.* (10) for details about extracting river width from JERS-1 SAR images). Fig. 3 shows three SAR images of the Pakse region corresponding to low, middle and flood periods respectively, which indicate that variations of discharge can be traced by the change of water surface area. A total of 16 river width records were obtained, which were used as calibration data for the integrated model. A good correlation ($W_e = 1221.3Q^{0.0341}$, $R^2=0.92$) exists between the 16 width records and the gauged discharge at the Pakse station.

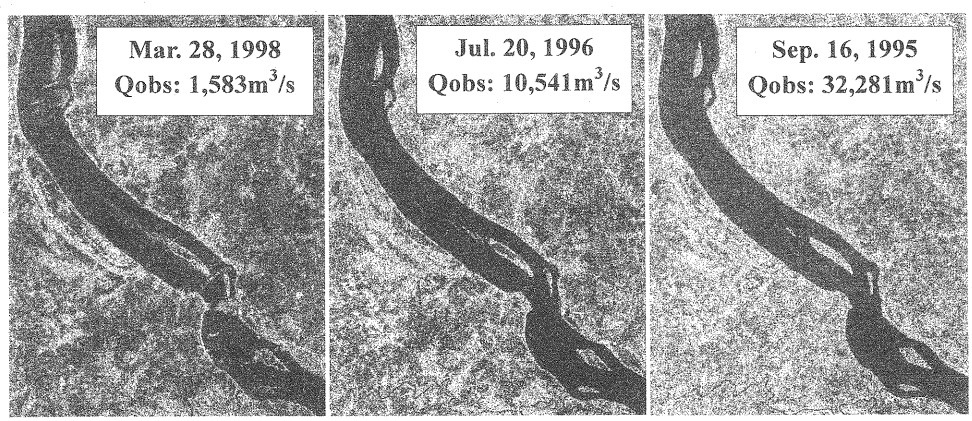

Fig. 3 Three SAR images for different flow period at Pakse region and corresponding measured discharge

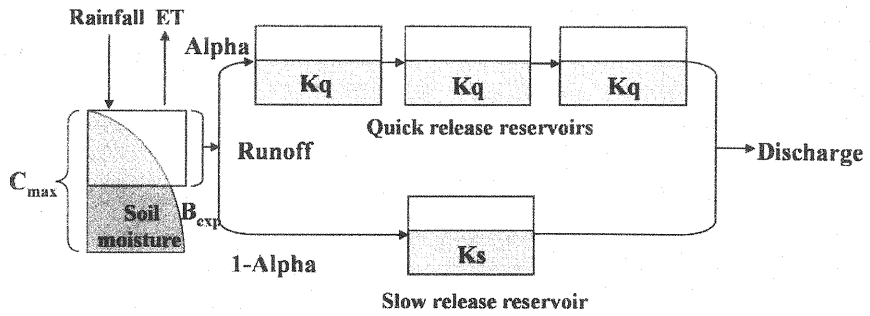

Fig. 4 Schematic description of HYMOD's structure

RR model

HYdrological MODel (HYMOD) is a parsimonious daily step model developed by Boyle (11), based on probability distributed model proposed by Moore (12). As shown in Fig. 4, it has a nonlinear soil moisture accounting component connected to a linear routing system that consists of a series of three identical quick release reservoirs in parallel with one slow release reservoir. There are five parameters: C_{max} is the maximum soil moisture storage capacity; B_{exp} is the degree of spatial variability of the soil moisture capacity; Alpha is the factor distributing the flow between slow and quick release reservoirs; Ks and Kq are the residence time of the slow release reservoir and quick release reservoirs respectively. To apply HYMOD to large basins, the whole basin was divided into subbasins to describe more accurately spatial variations, and two routing parameters were spatially varied depending on the distance between each subbasin and basin outlet. The upstream area of the Pakse station was divided into eight subbasins. Input data included daily rainfall data of the period of 1995-1998 from 26 gauging stations and Ahn and Tateishi potential evapotranspiration (representative of 1920-1980) (13).

Extracting river cross-sectional geometry from PRISM DSM

To reduce measurement error and approximate the mean conditions at Pakse region, for measuring river width from JERS-1 SAR images, river width being measured is average width over certain reach length. For similar reasons, the *W-H* relations of 30 cross-sections measured from DSM were averaged to reflect regional condition. Locations of the cross-sections are shown in Fig. 5. The distance between the two adjacent cross-sections is around 500 meter.

The DSM was generated from panchromatic images obtained on March 31, 2009. It was almost at the end of dry season. Therefore, most of the cross section can be measured from DSM. The elevations of the pixels adjacent to water surface were derived from DSM. The average elevation for the pixels on the left bank and right bank is 60.98 m (σ: 1.95 m) and 60.87 m (σ: 2.53 m) respectively. Considering the precision of DSM data (1 m), the value of 61 m was treated as an estimate of water surface elevation. Then the *W-H* relation of each cross-section for the portion above 60m was derived. At each integer elevation value, the average width of the 30 cross-sections was computed to form an average W-H relation in Pakse region. Fig. 6 shows the *W-H* relations of the 30 cross-sections derived from DSM individually and the average relation. A single linear function is utilized to describe this averaged regional relation:

$$W = \alpha H + \beta \tag{4}$$

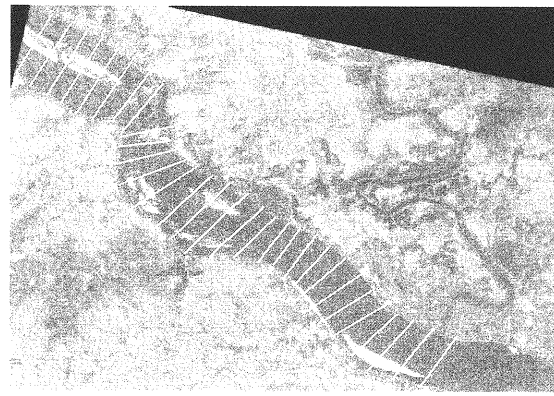

Fig. 5 Locations of 30 cross-sections at Pakse for which *W-H* relation is measured from DSM are shown on the ortho-rectified nadir image in the standard DSM product

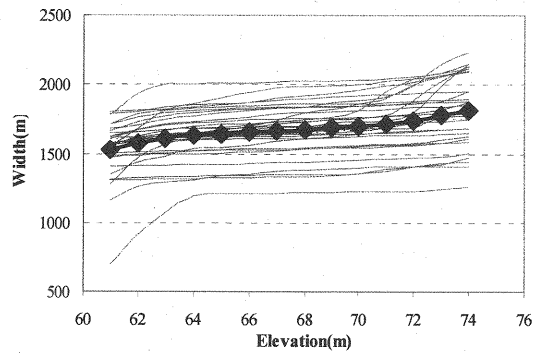

Fig. 6 The *W-H* relations derived from DSM data for the 30 cross-sections (gray lines) and the average relation (the thick black line with diamonds)

based on linear regression, value of α and β is 17.606 and 485.68m respectively. And the correlation is high (R^2= 0.95), which indicate assumption of linear relation is reasonable. In Pakse region, only in bank flow exists. Under assumption of symmetrical trapezoidal shape, the W_e-A and W_e-R relation is calculated from the regional *W-H* relation as follow respectively:

$$A = \frac{1}{2\alpha} \times \left[W_e^2 - (\alpha H_0 + \beta)^2 \right] \tag{5}$$

$$R = \sqrt{1+\frac{4}{\alpha^2}} \times W_e + \left(1 - \sqrt{1+\frac{4}{\alpha^2}} \right) \times (\alpha H_0 + \beta) \tag{6}$$

Incorporating Eqs. 5 and Eqs. 6 with Manning Equation, an explicit form of Eqs. 2 is obtained. As the explicit form of Eqs. 3 can not be derived, to calculate W_e corresponding to simulated discharge, the Newton-Raphson iteration method was applied to Eqs. 2. The values of n, S and H_0 were generated by using an automatic calibration algorithm, which were treated as known constants during the process of iteration.

Calibration algorithm

To reduce the RR model's parameter uncertainty, a multi-criteria method is considered as an effective approach (14). For the case study, only information from 16 time steps is available for calibration. A visual comparison between observed and simulated hydrograph was impossible. A multi-objective calibration algorithm: the Nondominated Sorting Genetic Algorithm II (NSGAII) was used. NSGAII is characterized as a fast nondominated sorting procedure, an elitist strategy, a parameterless approach and a simple yet efficient constraint-handling method (15). The fitness assignment is based on the Pareto ranking. And diversity maintenance is based on the crowing distance operator. The root mean square error (*RMSE*) and the coefficient of determination (R^2) were selected as objective functions. The calibration period for the integrated model was 1995-1998. The calibration under NSGAII attempted to find the locations in the parameter spaces that minimize the difference between the simulated width and the ones observed from remote sensing. Then the calibrated HYMOD alone was utilized for discharge estimation for the same period as calibration. To reduce the uncertainty in discharge estimation, the entire set of the plausible value of model parameters lying in the Pareto optimal front were all used to make prediction. At each time step, the average value of the discharge estimates made by the parameter sets was considered as a reliable estimate at that time step.

For the application of NSGAII, besides HYMOD's parameters, ranges for parameters in Eqs. 3 also need to be specified. For n, S and H_0, robust ranges which must be broad enough to ensure that model behaviors will span the range of observations can be obtained from literatures or estimated from limited local information. The range for n is literature range for alluvial, sand bedded channels with no vegetation (16). Based on longitudinal variations of the average bed elevation in the mainstream of the lower Mekong River observed by the COE Program of University of Yamanashi (17) in 2005, the river bed slope in Pakse region is very low (2.42×10^{-5}). Therefore, we set a relative low value for the upper bound of S. The average elevation for the pixels adjacent to water surface in DSM is 61m. We consider this value as the mean water surface elevation for the Pakse region at the moment that the PRISM images were captured. And H_0 should be lower than this value. Table 2 illustrates the range for the parameters of HYMOD and Eqs. 3 for the automatic optimization.

Table 2 Ranges of parameters need calibration

Parameter	Range	Parameter	Range
Cmax	200-400	*Kq*	0.5-2
Bexp	0.4-7	*n*	0.017-0.035
Alpha	0.2-0.99	*S*	0-0.02
Ks	0.01-0.5	H_0	55-63

RESULTS AND DISCUSSION

River discharge estimation

With parameter sets lying in the Pareto optimal front, after calibration, HYMOD alone was applied for discharge estimation for the same period as calibration. The average Nash coefficient was 89.98%. Fig. 7 shows the average simulated discharge and observations at Pakse. Most parts of hydrograph are well reproduced well by simulation. To quantitively assess the accuracy, the numbers of discharge estimates within different levels of relative error are shown in Table 3 in the form of percentages.

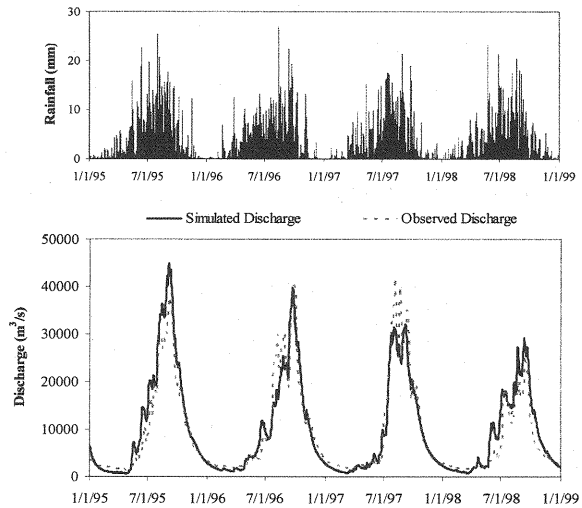

Fig. 7 Basin averaged rainfall, observed discharge at Pakse station and discharge estimated from calibration based on river width for 1995-1998

Table 3 Percentage of daily discharge estimates within different levels of relative error

Levels of Relative Error	±0.1	±0.2	±0.5	±1.0
Percentage of Estimates	25%	44%	83%	97%

The S, H_0, n obtained from calibration

Compared with the calibration scheme adopted by Sun *et al.* (10), one advantage is that S and H_0 describing the Q-W_e relation at the basin outlet are physically meaningful. From another point of view, the effectiveness of the method proposed can be justified by the value of S, H_0, n obtained from calibration, which is 1.16×10^{-4}, 60.93m, 0.0272 respectively. Fig. 8 shows the relation between the gauged water surface slope and the corresponding observed daily discharge in the Pakse region for the period of 1999-2000. The calibrated value is within the range of observations. The DSM was observed at the end of dry season. The water surface elevation is expected to be the lowest in a year. The difference between the calibrated H_0 and the water surface elevation measured from DSM is 0.07m (61m minus 60.93m), which reflect the fact that on that day, the water depth was quite shallow. By considering the precision of DSM (one meter), we conclude that the calibrated value for H_0 is also reasonable.

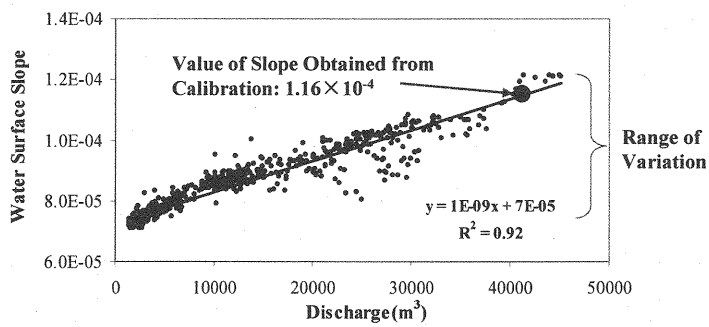

Fig. 8 Relation between observed discharge and water surface slope at Pakse region

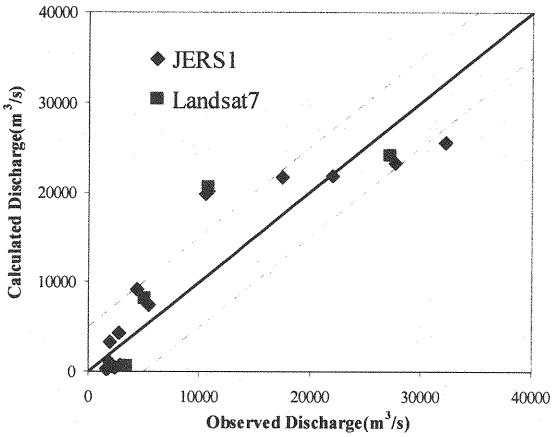

Fig. 9 Estimated discharge plotted against observed discharge based on Eqs. 2 for width records derived from 16 scenes of JERS-1 images and 4 scenes of Landsat7 images. The plots embraced by the dashed line are the ones that estimation error is less than 5,000 m^3/s.

To validate the value of n, we applied Eqs. 2 to estimate discharge directly, based on the parameters values obtained from calibration, W_e-R and W_e-A relations extracted from DSM. Discharges corresponding to river width records measured from the 16 JERS-1 SAR images and additional 4 Landsat7 images for the period of 1999-2002 were calculated. As the imaging mechanism for JERS-1 and Landsat7 are different, we consider characteristics of error for width measurements from the two sets of images should be different. However, the error of discharge estimates reveals similar trends as shown in Fig. 9: in high flow and low flow range, discharge is under estimated; and it is over estimated in middle flow range. Similar trends for both sets of images illustrate that the impact of error in width measurement is minor. The uncertainty associated with using Eqs. 2 to describe hydraulic conditions for the Pakse region is the main reason for error in discharge estimation.

For the low flow period, the discharge estimates are sensitive to H_0, which contribute to hydraulic variability that is highest in low flow period because of the effect of bedform and other types of channel irregularity (18). Variation of water surface slope for the reach in the Pakse region is low and the calibrated value corresponds to the high flow period as shown in Fig. 8. Dingman (4) suggests that a characteristic constant channel slope is hydraulically meaningful for certain reaches when estimating discharge with a general slope-resistance equation. As for the Manning coefficient, the general understanding is that it decreases as flow increases. The tendency of error in Fig. 9 indicates that the n obtained from calibration is lower than real situation for middle flow and overestimate the resistance for high flow period. Because this value is thought to reflect the average friction characteristic at the basin outlet for the whole calibration period, we consider it to be reasonable if judged from the viewpoint of calibration scheme.

CONCLUSIONS

This study is a first attempt to combine river cross-sectional geometry derived from high resolution DSM with the Manning Equation to describe Q-W_e relation. It was adopt to describe the hydraulic relation at the basin outlet, which facilities calibrating the RR model in basins that only satellite observations of river width are available at basin outlet. The results of case study show that most parts of hydrograph are well reproduced by the calibrated RR model. Also the calibrated values for S, H_0, n properly reflects hydraulic conditions for the whole calibration period. In

conclusion, the method provides a new approach to the application of the RR model in ungauged basins, using very limited information for the basin outlet derived from remote sensing as a surrogate for discharge data. For further validation of this concept, uncertainty associated with the error of DSM needs to be analyzed. This requires ground observation of the cross-sectional shape for comparison. Under the current calibration scheme, the Manning coefficient is treated as a time-invariant parameter. To represent the hydraulic relation at the basin outlet more accurately, it is desired to making the Manning coefficient as a dynamic parameter.

ACKNOWLEDGEMENTS

The authors sincerely acknowledge MEXT Grand-in-aid Scientific Research (No.21560537, PI: H. Ishidaira, University of Yamanashi) and the Global COE Program of University of Yamanashi for supporting this study.

REFERENCES

1. Alsdorf, D.E. and Lettenmaier D. P.: Tracking fresh water from space, Science, Vol.301, pp.1485-1488, 2007.
2. Vörösmarty, C., Birkett C., Dingman S.L., Lettenmaier D.P., Kim Y., Rodriguez E., Emmitt G.D., Plant W. and Wood E.S.: NASA post-2002 land surface hydrology mission component for surface water monitoring, HYDRA-SAT, Report from the NASA Post 2002 LSHP Planning Workshop, Irvine, pp.53, 2002.
3. Barrett, E.: Satellite remote sensing in hydrometry: Hydrometry: Principles and Practices, Herschy, R.W. eds., Wiley, pp.199-224, 1998.
4. Dingman, S.L. and Bjerklie, D.M.: Estimation of river discharge: Encyclopedia of hydrological science, Anderson M.G. eds., John Wiley &Sons, Ltd., 2005.
5. Smith, L. C., Isacks, B. L., Forster, R. R., Bloom, A. L. and Preuss, I.: Estimation of discharge from braided glacial rivers using ERS 1 synthetic aperture radar: First results, Water Resources Research., Vol.31, No.5, pp.1325-1329, 1995.
6. Coe, M. T. and Birkett C. M: Calculation of river discharge and prediction of lake height from satellite radar altimetry: Example for Lake Chad basin, Water Resources Research., Vol.40, No.10, pp.W102051-W1020511, 2004.
7. Bjerklie, D. M., Moller, D., Smith, L. C. and Dingman, S. L.: Estimating discharge in rivers using remotely sensed hydraulic information, Journal of Hydrology, Vol.309, pp.191-209, 2005.
8. Smith, L.C., Isacks, B.L., Bloom, A.L. and Murray, A.B.: Estimation of discharge from braid rivers using synthetic aperture radar imagery: Potential application to ungauged basins, Water Resources Research, Vol.32, pp.2021-2034, 1996.
9. Takaku, J. and Tadono, T.: PRISM geometry validation and DSM generation status, Proceeding of the First Joint PI Symposium of ALOS Data Nodes for ALOS Science Program in Kyoto, 2007.
10. Sun, W.C., Ishidaira, H. and Bastola, S.: Estimating discharge by calibrating hydrological model against water surface width measured from satellites in large ungauged basins, Annual Journal of Hydraulic Engineering, JSCE, Vol.53, pp.49-54, 2009.
11. Boyle, D. P.: Multicriteria calibration of hydrological models, Ph.D.Thesis, University of Arizona, USA, 2000.
12. Moore, R.J.: The probability-distributed principle and runoff production at point and basin scales, Hydrological Science Journal., Vol.30, No.2, pp.273-297, 1995.
13. Ahn, C.-H. and Tateishi, R.: Development of a global 30-minute grid potential evapotranspiration data set, Journal

of the Japan Society of Photogrammetry and Remote Sensing, Vol.33, No.2, pp.12-21, 1994.

14. Gupta, H.V., Beven, K.J. and Wagener, T.: Model calibration and uncertainty estimation: Encyclopedia of hydrological science, Anderson M.G. eds., John Wiley &Sons, Ltd., 2005.
15. Deb, K., Pratap, A., Agarwal, S. and Meyarivan, T.: A fast and elitist multiobjective genetic algorithm: NSGA-II, IEEE Transactions on Evolutionary Computation, Vol.6, No.2, pp.182-197, 2002.
16. Albertson, M.L. and Simons, D.B.: Fluid mechanics: Handbook of Applied Hydrology, Chow V.T. eds., McGraw-Hill, New York, 1964.
17. Morphological Characteristics of Lower Mekong River Project (MCLMR Project) Report, the 21st Century COE Program, University of Yamanashi, Japan, 2005.
18. Stewardson, M.: Hydraulic geometry of stream reaches, Journal of Hydrology, Vol.306, pp.97-111, 2005.

(Received Aug, 01, 2010 ; revised Dec, 22, 2010)